

# Nonequilibrium Weak Processes in Kaon Condensation I

## — Reaction rate for the thermal kaon process —

Takumi Muto\*

*Department of Physics, Chiba Institute of Technology, 2-1-1 Shibazono, Narashino, Chiba 275-0023, Japan*

Toshitaka Tatsumi†

*Department of Physics, Kyoto University, Kyoto 606-8502, Japan*

Naoki Iwamoto‡

*Department of Physics and Astronomy, The University of Toledo, Toledo, Ohio 43606-3390, U.S.A.*

### Abstract

We investigate the thermal kaon process, in which kaons are thermally produced via nucleon-nucleon collisions. This process is relevant to nonequilibrium dynamics of kaon condensation inside neutron stars. The reaction rates for these processes are calculated, and their temperature and density dependences are compared with those of other reaction rates. It is shown that the thermal kaon process is dominant over other relevant weak reactions throughout the nonequilibrium process, such as the kaon-induced Urca and the modified Urca reactions, and may control the entire evolution of the kaon condensate. The characteristic role of the soft and hard kaons during the evolution is explained, and implications for astrophysical phenomena are briefly discussed.

---

\*p21mutot@cc.it-chiba.ac.jp

†tatsumi@ruby.scphys.kyoto-u.ac.jp

‡iwamoto@uoft02.utoledo.edu

## I. INTRODUCTION

Modifications of properties of hadrons in a hot and/or dense nuclear medium have been an important subject in nuclear physics. Specifically, kaon condensation has attracted much interest as a possible new hadronic phase in the context of astrophysics and heavy-ion physics [1–4]. This condensate represents a Bose-Einstein condensation (BEC) of the negatively charged kaons ( $K^-$ ), driving force for which comes mainly from the  $s$  wave kaon-nucleon ( $KN$ ) attractions, i.e., the scalar interaction (the  $KN$  sigma term) and the vector interaction (the Tomozawa-Weinberg term) [2,3]. Kaon condensation may also be characterized as a macroscopic appearance of strangeness, which may have a close connection to strange matter. Based on experiments, the nature of attractive in-medium antikaon-nucleon interaction has recently been studied extensively in antikaon-nucleon scattering [5,6], in kaonic atoms [7], and in kaon-antikaon production via relativistic nucleus-nucleus collisions [8–10]. In particular, the experimental data for kaon-antikaon subthreshold production indicate a substantially reduced in-medium antikaon effective mass, which agrees with theoretical predictions [9]. Thus, the basic theoretical idea of kaon condensation seems to be gaining experimental support.

Most of the discussions about kaon condensation so far have been focused on equilibrium properties of dense matter at low temperature: The appearance of a kaon-condensed phase in neutron stars would lead to softening of the equation of state (EOS) [11]. Its presence also brings about rapid cooling of neutron stars [12,13]. Recently, studies have been made of the possibility of a delayed collapse of protoneutron stars to low-mass black holes [14–18], possibly caused by the softening of EOS by hadronic phase transitions during the evolution of protoneutron stars. In this case kaon condensation should appear in the high temperature and/or neutrino trapping situations. The equation of state for isothermal and isentropic cases and the properties of protoneutron stars with kaon condensation have been studied on the basis of chiral symmetry [19,20]. However, the formation of a kaon condensate from noncondensed matter and its evolution involve *weak reaction processes* that change strangeness, so that it takes some time for chemical equilibrium to be reached: the typical time scale of the weak reactions is much longer than those for the strong and electromagnetic interactions, and is also different from the typical time scale for gravitational collapse (of order of a millisecond) and that for deleptonization and initial cooling (of order of a second). Therefore, the nonequilibrium weak processes may have an important effect on the dynamical evolution of kaon-condensed stars just after supernova explosions.

Basic concept of nucleation in BEC is applied to a wide range of systems besides kaon condensation [21]. Concerning the nonequilibrium dynamics and the formation time of BEC, theoretical works have been carried out for a weakly interacting Bose gas [22], prior to the first experimental achievements of BEC in alkali atoms [23]. In atomic gases, the energy of the atoms is little affected by the weakly repulsive interaction between the atoms, and the same interaction controls the onset and the build-up time scales of the condensate with the number of atoms fixed. On the other hand, the system of kaons and nucleons (which we call the  $KN$  system) is unique in the following respects: The microscopic quantities in the  $KN$  system, such as the energies of the particles, are determined by the strong and electromagnetic interactions between the kaons, baryons and leptons. In particular, the kaons couple to the nuclear medium via strong interactions, and the kaon excitation energy is reduced primarily by  $s$ -wave  $KN$  attractive interactions. The time scales for these interactions are much shorter than those of weak interactions, so that

the  $KN$  system is likely to be in thermal equilibrium during the chemical-nonequilibrium processes brought about by the weak reactions. As a result, the chemical-nonequilibrium state evolves adiabatically, adjusting to the gradual change of the chemical composition, which is determined by the kinetic equations induced by the weak reactions. The relevant such reactions are given by

$$n + n \rightarrow n + p + K^-, \quad (1a)$$

$$n + p + K^- \rightarrow n + n, \quad (1b)$$

where the presence of a spectator neutron is necessary in order to satisfy the kinematical conditions in a degenerate Fermi system. (We call these reactions thermal kaon process, and denote it as KT. ) Other weak reactions are given by the kaon-induced Urca process (KU) [12],

$$n(p) \rightarrow n(p) + e^- + \bar{\nu}_e, \quad (2a)$$

$$n(p) + e^- \rightarrow n(p) + \nu_e, \quad (2b)$$

and the modified Urca process (MU) [24,25],

$$n + n \rightarrow n + p + e^- + \bar{\nu}_e, \quad (3a)$$

$$n + p + e^- \rightarrow n + n + \nu_e. \quad (3b)$$

Alternatively, the KU process (2) may be written symbolically as  $n(p) + \langle K^- \rangle \rightarrow n(p) + e^- + \bar{\nu}_e$ ,  $n(p) + e^- \rightarrow n(p) + \langle K^- \rangle + \nu_e$ , in terms of the condensate  $\langle K^- \rangle$ . It is to be noted that the KU process is operative only in the presence of a condensate, so that, in the noncondensed (normal) phase, only the KT and the MU processes proceed. Thus kaons, as quasiparticles whose properties are modified by the medium effects, are emitted and absorbed through the weak reactions (1) and (2), and the total number of kaons (and the corresponding strangeness in the medium) changes during the nonequilibrium weak processes. It is these weak reactions that determine the characteristic time scales of the system. <sup>1</sup>

In [27], we have discussed the nonequilibrium processes in a kaon condensate by taking into account only the KU and the MU reactions, and assuming the presence of a small seed of condensate. However, in thermal equilibrium, the onset of condensation can occur naturally without a seed when the KT reactions are included: specifically, once the thermal kaon density is saturated, kaons are created thermally and then converted to a condensate. In a series of our works, we take into account the thermal kaon process KT as well as KU and MU, and consider the effects of thermal kaons on the kinetics of kaon condensation during the whole nonequilibrium process. In this paper (paper I), we mainly consider the reaction rates for the thermal kaon process (1). We present a unified description of the excitation energy of kaons and the weak interactions based on chiral symmetry. In a subsequent paper (paper II) [28], the time dependent behavior of the physical quantities, such as the amplitude of the condensate, number densities of the chemical species, will be discussed, based on the results of this paper.

---

<sup>1</sup>Concerning strangeness production, some authors considered strange quark matter, where the nonleptonic weak reactions,  $u+d \rightleftharpoons s+u$ , together with the semileptonic ones,  $d(s) \rightarrow u+e^-+\bar{\nu}_e$ ,  $u+e^- \rightarrow d(s)+\nu_e$ , have been taken into account [26]. One can see a similarity in these weak reactions between strange matter and kaon condensation.

This paper is organized as follows: The expressions for the reaction rates are obtained in Sec.II. Sec.III outlines the physical properties of the nonequilibrium process. In Sec.IV, the numerical results are presented, and temperature and the density dependences of these reaction rates are compared with other reaction rates. Summary and concluding remarks are given in Sec.V. The expressions for other weak reaction rates for KU and MU are outlined in Appendix A.

## II. FORMULATION

### A. Brief survey of the chiral symmetry approach

We first give an outline of the kaon-condensed state on the basis of chiral symmetry. In the framework of the  $SU_L(3) \times SU_R(3)$  current algebra and PCAC, the  $s$ -wave  $K^-$  condensed state,  $|K^- \rangle$ , is generated by a chiral rotation of the normal state  $|0 \rangle$  as  $|K^- \rangle = \hat{U}_K |0 \rangle$ , with the unitary operator  $\hat{U}_K$  given by

$$\hat{U}_K \equiv \exp(i\mu_K t Q) \exp(i\theta Q_4^5), \quad (4)$$

where  $\mu_K$  is the kaon chemical potential,  $\theta$  the chiral angle which represents the order parameter of the system, and  $Q$  ( $Q_4^5$ ) the electromagnetic charge operator (the axial charge operator). The classical  $K^-$  field is then given as

$$\langle K^- \rangle \equiv \langle K^- | \hat{K}^- | K^- \rangle = \langle 0 | \hat{U}_K^{-1} \hat{K}^- \hat{U}_K | 0 \rangle = \frac{f}{\sqrt{2}} \sin \theta \exp(-i\mu_K t), \quad (5)$$

where  $f$  (=93 MeV) is the meson decay constant.

### B. Reaction rate for thermal kaon process

Here we consider the kaon-producing (forward) reactions (1a).<sup>2</sup> The lowest-order diagrams are given in Fig.1, where  $a - c$  represent the direct diagrams and  $a' - c'$  the exchange diagrams. In Fig.1, lines 1 and 2 denote the neutrons in the initial state, and lines 3 and 4, the proton and the neutron in the final state, respectively. The scattering of two nucleons is treated in terms of the one-pion exchange potential (OPEP) which represents the long-range nuclear interaction. The medium and short-range interactions, which are mediated by heavier mesons, are neglected here.<sup>3</sup>

The reaction rate per unit volume is given in terms of the transition rate  $W_{\text{fi}}$  by

$$\Gamma^{(\text{KT-F})} = \frac{2\pi}{(2\pi)^{15}} \int d^3 p_1 \int d^3 p_2 \int d^3 p_3 \int d^3 p_4 \int d^3 p_K \delta(E_f - E_i) W_{\text{fi}} S, \quad (6)$$

where  $S$  is the statistical factor,  $S = \frac{1}{s} n(\mathbf{p}_1) n(\mathbf{p}_2) [1 - n(\mathbf{p}_3)] [1 - n(\mathbf{p}_4)] [1 + f_{K^-}(\mathbf{p}_K)]$ , with the symmetry factor  $s$  (=2),  $n(\mathbf{p}_i)$  ( $i = 1 - 4$ ) the Fermi-Dirac distribution function for the nucleon, and  $f_{K^-}(\mathbf{p}_K)$  the Bose-Einstein distribution function for the  $K^-$ . The nucleons and the kaons are assumed to be in thermal equilibrium.

<sup>2</sup> Throughout this paper, we use the units in which  $\hbar = k_B = 1$ .

<sup>3</sup> We simply follow the treatment for the nuclear interaction adopted in ref. [25].

### C. Matrix elements

The transition rate  $W_{\text{fi}}$  is written as

$$W_{\text{fi}} = (2\pi)^3 \delta^{(3)}(\mathbf{p}_3 + \mathbf{p}_4 + \mathbf{p}_K - \mathbf{p}_1 - \mathbf{p}_2) \sum_{\text{spins}} |M|^2, \quad (7)$$

where  $|M|^2$  is the squared matrix element, and the summation is over the initial and final nucleon spins.

The effective weak Hamiltonian is of the current–current interaction type,  $H_W = \frac{G_F}{\sqrt{2}} J_h^\mu \cdot J_{h\mu}^\dagger + \text{h.c.}$  with the charged hadronic current,  $J_h^\mu = \cos\theta_C(V_{1+i2}^\mu - A_{1+i2}^\mu) + \sin\theta_C(V_{4+i5}^\mu - A_{4+i5}^\mu)$ , where  $\theta_C (\simeq 0.24)$  is the Cabibbo angle, and  $V_a^\mu$  and  $A_a^\mu$  are the vector and axial vector currents, respectively.

In the kaon-condensed state  $|K^- \rangle$ , the matrix elements must be evaluated from the transformed Hamiltonian [12,13]

$$\widetilde{H}_W = \hat{U}_K^{-1} H_W \hat{U}_K = \frac{G_F}{\sqrt{2}} \widetilde{J}_h^\mu \widetilde{J}_{h\mu}^\dagger + \text{h.c.}, \quad (8)$$

where the effective hadronic current  $\widetilde{J}_h^\mu$  is given in a model-independent form by way of current algebra:

$$\begin{aligned} \widetilde{J}_h^\mu &= \hat{U}_K^{-1} J_h^\mu \hat{U}_K \\ &= e^{-i\mu_K t} \left[ \cos\theta_C \left\{ (V_{1+i2}^\mu - A_{1+i2}^\mu) \cos(\theta/2) + i(V_{6-i7}^\mu - A_{6-i7}^\mu) \sin(\theta/2) \right\} \right. \\ &\quad \left. + \sin\theta_C \left\{ (V_4^\mu - A_4^\mu) + i \cos\theta (V_5^\mu - A_5^\mu) - \frac{i}{2} \sin\theta (V_3^\mu - A_3^\mu + \sqrt{3}(V_8^\mu - A_8^\mu)) \right\} \right]. \quad (9) \end{aligned}$$

Then the relevant isospin-changing strangeness-conserving nucleon current can be read off from (9) in the nonrelativistic form as

$$\widetilde{J}_N^\mu = e^{-i\mu_K t} \cos\theta_C \cos\frac{\theta}{2} \chi^\dagger(p) (\delta_0^\mu - g_A \delta_i^\mu \sigma^i) \chi(n) \quad (10)$$

with the two-component Pauli spinor  $\chi(N)$  for the nucleon and  $g_A (=1.25)$  the axial-vector coupling strength. The kaon sector in the hadronic current is implemented in the isospin and strangeness-changing axial vector terms in (9), and may be written as

$$\widetilde{J}_K^\mu = -e^{-i\mu_K t} \sin\theta_C \left( \cos^2\frac{\theta}{2} j_{K^-}^\mu + \sin^2\frac{\theta}{2} j_{K^+}^\mu \right) \quad (11)$$

with  $j_{K^\pm}^\mu \equiv A_4^\mu \mp iA_5^\mu$ . In (11), the first term in the bracket contributes to the thermal  $K^-$  process. The kaon current  $j_{K^\pm}^\mu$  may be determined from the PCAC ansatz,  $\partial_\mu j_{K^\pm}^\mu = \sqrt{2} f m_K^2 K^\pm$ ,<sup>4</sup> so that we take

$$j_{K^\pm}^\mu = \sqrt{2} f \partial^\mu K^\pm = \pm i \sqrt{2} f \frac{(p_{K^\pm})^\mu}{\sqrt{2\omega_\pm}} \exp(\pm i p_{K^\pm} x), \quad (12)$$

---

<sup>4</sup> Generally speaking, the kaon current consists of a free kaon part and a kaon-baryon interaction part.

where  $(p_{K^\pm})^\mu = (\omega_\pm, \mathbf{p}_{K^\pm})$  is the kaon four-momentum with energy  $\omega_\pm$ . In a nuclear medium, the dispersion relations for the kaons,  $\omega_\pm(\mathbf{p}_{K^\pm})$ , differ from those in vacuum. See Sec.III for the explicit expression for  $\omega_\pm$ .

For the pion-nucleon interaction, we take the pseudovector -coupling Lagrangian:

$$\mathcal{L}_{\pi NN} = \tilde{f}\tilde{\Psi}\gamma^\mu\gamma_5\tau_a\Psi\partial_\mu\varphi_a + \text{h.c.} , \quad (13)$$

where  $\tilde{f} \equiv f_{\pi NN}/m_\pi$ , with  $f_{\pi NN}$  the  $\pi NN$  coupling constant,  $m_\pi(=140 \text{ MeV})$  the pion mass,  $\Psi$  the nucleon isodoublet, and  $\varphi_a$  the pion isotriplet.

The diagrams in Fig.1 are similar to those in the modified Urca (MU) process (3). The only difference between these processes is that a lepton pair  $e^-\bar{\nu}_e$  in MU is replaced by a kaon in KT. Thus, the matrix element for KT can be obtained by a replacement of the  $npe^-\bar{\nu}_e$  vertex factor in MU by a  $npK^-$  vertex factor. In addition, the KT and MU reactions differ in the statistical factor  $S$  [ see Eq.(6) for KT ], as a result of the different statistics of the participating particles. From (8)–(12), the vertex factor can be read as  $\frac{G_F}{\sqrt{2}} \cos\theta_C K_\mu(\delta_0^\mu - g_A\delta_i^\mu\sigma^i)$ , where

$$K_\mu \equiv -if \sin\theta_C \frac{(p_K)_\mu}{\omega_-^{1/2}} \cos^3\frac{\theta}{2} . \quad (14)$$

The remaining assignments in the matrix elements of Fig.1 are made with reference to Friman and Maxwell's result for the MU process [24,25]:

(i) A factor  $-\tilde{f}\boldsymbol{\sigma}\cdot\mathbf{k}$  for the  $nn\pi^0$  vertex, a factor  $\tilde{f}\boldsymbol{\sigma}\cdot\mathbf{k}$  for the  $pp\pi^0$  vertex, and a factor  $\sqrt{2}\tilde{f}\boldsymbol{\sigma}\cdot\mathbf{k}$  for the  $np\pi^-$  vertex, where  $\mathbf{k}$  is the pion momentum.

(ii) A factor  $-1/(\mathbf{k}^2 + m_\pi^2)$  for the pion propagator .

(iii) A nucleon propagator  $iG$  at the nucleon internal line, which, when the kaon couples to the outgoing (incoming) nucleon, is given by  $i/(E_p + \omega_- - E_n)$  ( $i/(E_n - E_p - \omega_-)$ ), where  $E_N$  is the single particle energy of the nucleon. The nucleon propagator is further expanded in powers of the inverse nucleon mass, and only the lowest order term is retained, so that  $iG \sim i/\omega_-$  ( $iG \sim -i/\omega_-$ ).

Here we summarize the matrix element for each diagram for the kaon-producing KT process (1a). For the direct diagrams (a)–(c), one obtains

$$M^{(a)}(1, 2, 3, 4; l) = -i\frac{G_F}{\sqrt{2}} \cos\theta_C K_\mu \tilde{f}^2 \frac{1}{\omega_-} \frac{1}{\mathbf{l}^2 + m_\pi^2} \left\{ \chi_4^\dagger(\boldsymbol{\sigma}\cdot\mathbf{l})\chi_2 \cdot \chi_3^\dagger(\delta_0^\mu - g_A\delta_i^\mu\sigma^i)(\boldsymbol{\sigma}\cdot\mathbf{l})\chi_1 \right\} , \quad (15a)$$

$$M^{(b)}(1, 2, 3, 4; l) = -i\frac{G_F}{\sqrt{2}} \cos\theta_C K_\mu \tilde{f}^2 \frac{1}{\omega_-} \frac{1}{\mathbf{l}^2 + m_\pi^2} \left\{ \chi_4^\dagger(\boldsymbol{\sigma}\cdot\mathbf{l})\chi_2 \cdot \chi_3^\dagger(\boldsymbol{\sigma}\cdot\mathbf{l})(\delta_0^\mu - g_A\delta_i^\mu\sigma^i)\chi_1 \right\} , \quad (15b)$$

$$M^{(c)}(1, 2, 3, 4; k) = i\frac{G_F}{\sqrt{2}} \cos\theta_C K_\mu \cdot 2\tilde{f}^2 \frac{1}{\omega_-} \frac{1}{\mathbf{k}^2 + m_\pi^2} \left\{ \chi_4^\dagger(\boldsymbol{\sigma}\cdot\mathbf{k})(\delta_0^\mu - g_A\delta_i^\mu\sigma^i)\chi_2 \cdot \chi_3^\dagger(\boldsymbol{\sigma}\cdot\mathbf{k})\chi_1 \right\} , \quad (15c)$$

where  $k = p_1 - p_3$ ,  $l = p_4 - p_2$ .

For the exchange diagrams (a')–(c'), one obtains

$$\begin{aligned} M^{(a')} &= -M^{(a)}(2, 1, 3, 4; -k') \\ &= i\frac{G_F}{\sqrt{2}} \cos\theta_C K_\mu \tilde{f}^2 \frac{1}{\omega_-} \frac{1}{\mathbf{k}'^2 + m_\pi^2} \left\{ \chi_4^\dagger(\boldsymbol{\sigma}\cdot\mathbf{k}')\chi_1 \cdot \chi_3^\dagger(\delta_0^\mu - g_A\delta_i^\mu\sigma^i)(\boldsymbol{\sigma}\cdot\mathbf{k}')\chi_2 \right\} , \end{aligned}$$

(16a)

$$\begin{aligned}
M^{(b')} &= -M^{(b)}(2, 1, 3, 4; -k') \\
&= i \frac{G_F}{\sqrt{2}} \cos \theta_C K_\mu \tilde{f}^2 \frac{1}{\omega_-} \frac{1}{\mathbf{k}'^2 + m_\pi^2} \left\{ \chi_4^\dagger(\boldsymbol{\sigma} \cdot \mathbf{k}') \chi_1 \cdot \chi_3^\dagger(\boldsymbol{\sigma} \cdot \mathbf{k}') (\delta_0^\mu - g_A \delta_i^\mu \sigma^i) \chi_2 \right\},
\end{aligned}$$

(16b)

$$\begin{aligned}
M^{(c')} &= -M^{(c)}(2, 1, 3, 4; -l') \\
&= -i \frac{G_F}{\sqrt{2}} \cos \theta_C K_\mu \cdot 2 \tilde{f}^2 \frac{1}{\omega_-} \frac{1}{\mathbf{l}'^2 + m_\pi^2} \left\{ \chi_4^\dagger(\boldsymbol{\sigma} \cdot \mathbf{l}') (\delta_0^\mu - g_A \delta_i^\mu \sigma^i) \chi_1 \cdot \chi_3^\dagger(\boldsymbol{\sigma} \cdot \mathbf{l}') \chi_2 \right\},
\end{aligned}$$

(16c)

where  $k' = p_1 - p_4$ ,  $l' = p_3 - p_2$ .

From momentum conservation,  $\mathbf{k} = \mathbf{l} \pm \mathbf{p}_K$  and  $\mathbf{k}' = \mathbf{l}' \pm \mathbf{p}_K$ . Since the nucleons are degenerate, only those near the Fermi surfaces contribute to the relevant phase space of the reactions. Thus, the momenta for the nucleons in these relations may be replaced by the Fermi momenta, i.e.,  $\mathbf{p}_F(n)$  for  $\mathbf{p}_1$ ,  $\mathbf{p}_2$ , and  $\mathbf{p}_4$ , and  $\mathbf{p}_F(p)$  for  $\mathbf{p}_3$ . As we will see in Sec.IV, the proton Fermi momentum in the noncondensed state is estimated as  $|\mathbf{p}_F(p)| = 260\text{--}290$  MeV for the typical baryon number densities  $n_B = 0.55\text{--}0.70$  fm $^{-3}$ , whereas the corresponding neutron Fermi momentum is  $|\mathbf{p}_F(n)| = 470\text{--}510$  MeV. In addition, the typical value of the momentum of the thermal kaons which mainly contributes to the reactions is 120–180 MeV. Thus, both  $|\mathbf{p}_F(p)|$  and  $|\mathbf{p}_K|$  are small compared with  $|\mathbf{p}_F(n)|$  at least in the noncondensed stage. Therefore we, hereafter, make an approximation by omitting the proton and the kaon momenta in the momentum conservation, and we put  $\mathbf{k} = \mathbf{l} \simeq \mathbf{p}_F(n)$  and  $\mathbf{k}' = \mathbf{l}' \simeq -\mathbf{p}_F(n)$ . Within this approximation, one obtains

$$\begin{aligned}
M^{(a)} + M^{(b)} + M^{(c)} &= 2g_A \frac{G_F}{\sqrt{2}} \cos \theta_C \tilde{f}^2 \frac{1}{\omega_-} \frac{1}{|\mathbf{p}_F(n)|^2 + m_\pi^2} K_\mu \delta_i^\mu \\
&\cdot \left[ \chi_3^\dagger \chi_1 \cdot \chi_4^\dagger(\boldsymbol{\sigma} \cdot \mathbf{k}) \chi_2 (ik^i) - \chi_3^\dagger(\boldsymbol{\sigma} \cdot \mathbf{k}) \chi_1 \left\{ \chi_4^\dagger \chi_2 (ik^i) - \chi_4^\dagger(\boldsymbol{\sigma} \times \mathbf{k})^i \chi_2 \right\} \right] \quad (17)
\end{aligned}$$

and

$$\begin{aligned}
M^{(a')} + M^{(b')} + M^{(c')} &= 2g_A \frac{G_F}{\sqrt{2}} \cos \theta_C \tilde{f}^2 \frac{1}{\omega_-} \frac{1}{|\mathbf{p}_F(n)|^2 + m_\pi^2} K_\mu \delta_i^\mu \\
&\cdot \left[ \left\{ \chi_4^\dagger \chi_1 (ik'^i) - \chi_4^\dagger(\boldsymbol{\sigma} \times \mathbf{k}')^i \chi_1 \right\} \chi_3^\dagger(\boldsymbol{\sigma} \cdot \mathbf{k}') \chi_2 - \chi_4^\dagger(\boldsymbol{\sigma} \cdot \mathbf{k}') \chi_1 \cdot \chi_3^\dagger \chi_2 (ik'^i) \right]. \quad (18)
\end{aligned}$$

It can be checked that the expressions for these summed matrix elements (17) and (18) are consistent with those for the MU process obtained by Maxwell [25] by simple replacements of the weak lepton current  $l_\mu$  and the energy  $\omega$  of the lepton pairs in [25], by  $K_\mu$  and  $\omega_-$ , respectively.

It is to be noted that the nucleon vector current part of the matrix element for the diagram (c) ( (c') ), where a charged pion propagates between the nucleons, is larger by a factor of two and is opposite in sign as compared with those for (a) and (b) [ (a') and (b') ], where a neutral pion propagates. [ cf. (15) and (16). ] This is due to the differences in the isospin factors at the  $\pi NN$  vertices and in the sign attached to the nucleon propagator (see (iii) ) between (c) and (a) or (b) [ (c') and (a') or (b') ]. As a result, the contribution from the nucleon vector current vanishes after summing up the matrix elements for the three diagrams (a), (b) and (c) [ (a'), (b') and (c') ], and only the axial-vector part, proportional to  $g_A \delta_i^\mu$ , contributes, as seen in (17) and (18). One finds that the  $s$ -wave condensed kaon cannot be directly emitted in place of the thermal kaon in the KT reaction. This is because the relevant kaon current has the form  $j_{K^-}^\mu = \sqrt{2} f \partial^\mu \langle K^- \rangle = -i \mu_K f^2 \sin \theta e^{-i \mu_K t} \cdot \delta_0^\mu$ , where

the spatial component is zero, so that the condensed-kaon current does not couple to the nonrelativistic nucleon axial-vector current [ cf. (17) and (18)].

By the use of (17) and (18), the spin-summed squared matrix element  $\sum_{\text{spins}} |M|^2$ , with  $M = M^{(a)} + M^{(b)} + M^{(c)} + M^{(a')} + M^{(b')} + M^{(c')}$ , is obtained as

$$\begin{aligned} \sum_{\text{spins}} |M|^2 &= 8 \left( g_A G_F \tilde{f}^2 f \sin \theta_C \cos \theta_C \cos^3 \frac{\theta}{2} \right)^2 \frac{1}{\omega_-^3} \frac{1}{(|\mathbf{p}_F(n)|^2 + m_\pi^2)^2} \\ &\cdot \left[ |\mathbf{p}_F(n)|^2 \{ (\mathbf{p}_K \cdot \mathbf{k})^2 + (\mathbf{p}_K \cdot \mathbf{k}')^2 + 2|\mathbf{p}_K|^2 |\mathbf{p}_F(n)|^2 \} \right. \\ &+ \left\{ 5(\mathbf{k} \cdot \mathbf{k}') (\mathbf{p}_K \cdot \mathbf{k}) (\mathbf{p}_K \cdot \mathbf{k}') - 2|\mathbf{p}_F(n)|^2 (\mathbf{p}_K \cdot \mathbf{k}')^2 - 2|\mathbf{p}_F(n)|^2 (\mathbf{p}_K \cdot \mathbf{k})^2 \right. \\ &\left. \left. - |\mathbf{p}_K|^2 (\mathbf{k} \cdot \mathbf{k}')^2 + \{ \mathbf{p}_K \cdot (\mathbf{k} \times \mathbf{k}') \}^2 \right\} \right]. \end{aligned} \quad (19)$$

#### D. Phase space integrals

The phase space integrals appearing in (6) for the reaction rate  $\Gamma^{(\text{KT})}$  are separated into radial and angular parts via the relation  $\Gamma^{(\text{KT})} = AP$ , where

$$A \equiv \frac{1}{(2\pi)^{11}} \left( \frac{8}{3} g_A G_F \tilde{f}^2 f \sin \theta_C \cos \theta_C \cos^3 \frac{\theta}{2} \frac{|\mathbf{p}_F(n)|^2}{|\mathbf{p}_F(n)|^2 + m_\pi^2} \right)^2, \quad (20)$$

and

$$P \equiv \int_0^\infty |\mathbf{p}_1|^2 d|\mathbf{p}_1| \int_0^\infty |\mathbf{p}_2|^2 d|\mathbf{p}_2| \int_0^\infty |\mathbf{p}_3|^2 d|\mathbf{p}_3| \int_0^\infty |\mathbf{p}_4|^2 d|\mathbf{p}_4| \int_0^\infty |\mathbf{p}_K|^2 d|\mathbf{p}_K| \delta(E_f - E_i) \frac{|\mathbf{p}_K|^2}{\omega_-^3} S Q \quad (21)$$

with

$$Q \equiv \int d\Omega_1 \int d\Omega_2 \int d\Omega_3 \int d\Omega_4 \int d\Omega_K \delta^{(3)}(\mathbf{p}_3 + \mathbf{p}_4 + \mathbf{p}_K - \mathbf{p}_1 - \mathbf{p}_2). \quad (22)$$

For those kaons which are the main contributors to the reaction rate, the momentum  $|\mathbf{p}_K|$  is small enough to satisfy the condition,  $|\mathbf{p}_K| + |\mathbf{p}_F(p)| < |\mathbf{p}_F(n)|$ . Under this condition, one obtains  $Q \simeq 8(2\pi)^4 |\mathbf{p}_F(p)| / (|\mathbf{p}_1| |\mathbf{p}_2| |\mathbf{p}_3| |\mathbf{p}_4|)$ . After substituting this result into (21), we transform the variables for the nonrelativistic nucleons in  $P$  by way of the relation  $|\mathbf{p}_i| d|\mathbf{p}_i| = m_i^* dE_i$  ( $i = 1 - 4$ ) with  $m_i^*$  the effective nucleon mass. By the further change of variables :  $x_1 = (E_1 - \mu_n)/T$ ,  $x_2 = (E_2 - \mu_n)/T$ ,  $x_3 = -(E_3 - \mu_p)/T$ ,  $x_4 = -(E_4 - \mu_n)/T$ , where  $\mu_i$  ( $i = 1 - 4$ ) is the chemical potential and  $T$  the temperature, one obtains

$$P = \frac{1}{6} (m_n^*)^3 m_p^* T^3 \int_0^\infty |\mathbf{p}_K|^2 d|\mathbf{p}_K| \frac{[(\omega_- + \mu_p - \mu_n)/T] \cdot [(\omega_- + \mu_p - \mu_n)^2/T^2 + 4\pi^2]}{e^{(\omega_- + \mu_p - \mu_n)/T} - 1} \frac{|\mathbf{p}_K|^2/\omega_-^3}{1 - e^{-(\omega_- - \mu_K)/T}}. \quad (23)$$

In obtaining (23), we have made the approximation (valid at low temperature),  $-\mu_i/T \rightarrow -\infty$ , for the lower limit of the four integrals with respect to  $x_1 - x_4$ , and the following formula has been used [29]:



$$\begin{aligned}
& \int_{-\infty}^{\infty} dx_1 \int_{-\infty}^{\infty} dx_2 \int_{-\infty}^{\infty} dx_3 \int_{-\infty}^{\infty} dx_4 \delta(x_1 + x_2 + x_3 + x_4 - y) \frac{1}{1 + e^{x_1}} \frac{1}{1 + e^{x_2}} \frac{1}{1 + e^{x_3}} \frac{1}{1 + e^{x_4}} \\
&= \frac{1}{6} \frac{y(y^2 + 4\pi^2)}{e^y - 1}.
\end{aligned} \tag{24}$$

The value of  $\mu_n$  ( $\mu_p$ ) is taken to be 200–300 MeV (100–200 MeV) at the relevant densities where the kaon condensation is realized. As a consequence of the rapid convergence of the integrand in (24) for negative values of  $x_i$  produced by the exponentials arising from the statistical factor  $S$ , the low-temperature approximation should be valid for temperatures less than several tens of MeV.

For the remaining integral in (23), we introduce a dimensionless variable  $x \equiv |\mathbf{p}_K|/T$ . Combining Eqs. (20) and (23), and the definition of  $\Gamma^{(\text{KT-F})}$ , one obtains the final expression for  $\Gamma^{(\text{KT-F})}$ :

$$\begin{aligned}
\Gamma^{(\text{KT-F})}(\xi^{(\text{KT})}, T) &= \frac{512}{9(2\pi)^7} \left( g_A G_F \tilde{f}^2 f \sin \theta_C \cos \theta_C \cos^3 \frac{\theta}{2} \frac{|\mathbf{p}_F(n)|^2}{|\mathbf{p}_F(n)|^2 + m_\pi^2} \right)^2 |\mathbf{p}_F(p)| \\
&\times (m_n^*)^3 m_p^* T^5 I^{(\text{KT})}(\xi^{(\text{KT})}, T)
\end{aligned} \tag{25a}$$

$$= (4.0 \times 10^{30}) \left( \frac{|\mathbf{p}_F(p)|}{m_\pi} \right) \left( \frac{m_n^*}{m_N} \right)^3 \left( \frac{m_p^*}{m_N} \right) \cos^6 \frac{\theta}{2} T_9^5 I^{(\text{KT})}(\xi^{(\text{KT})}, T) \tag{25b}$$

(cm<sup>-3</sup> · s<sup>-1</sup>),

where  $T_9$  is the temperature in units of 10<sup>9</sup> K,  $\xi^{(\text{KT})} \equiv (\mu_K + \mu_p - \mu_n)/T$ , and

$$I^{(\text{KT})}(u, T) = \int_0^\infty dx f(x; u, T), \tag{26}$$

with

$$f(x; u, T) \equiv \frac{1}{6} \frac{x^4}{(\tilde{\omega}_-(x) + \mu_K/T)^3} \frac{(\tilde{\omega}_-(x) + u) [(\tilde{\omega}_-(x) + u)^2 + 4\pi^2]}{1 - e^{-\tilde{\omega}_-(x)}} \frac{1}{e^{\tilde{\omega}_-(x)+u} - 1} \tag{27}$$

where  $\tilde{\omega}_-(x) \equiv (\omega_-(x) - \mu_K)/T$ .

The factor  $T^5$  in (25) comes from the energy integrals for two incoming and two outgoing nucleons ( $T^4$ ), together with the energy-conserving delta function ( $T^{-1}$ ), the radial integral with respect to the kaon momentum ( $T^3$ ), and the factor  $|\mathbf{p}_K|^2/\omega_-^3$  in the matrix element ( $T^{-1}$ ). The integral  $I^{(\text{KT})}(\xi^{(\text{KT})}, T)$  also depends on  $T$ , so that the reaction rate  $\Gamma^{(\text{KT-F})}(\xi^{(\text{KT})}, T)$  in general has a complicated temperature dependence.

For the backward process (1b), the reaction rate  $\Gamma^{(\text{KT-B})}(\xi^{(\text{KT})}, T)$  can be given in a manner similar to the forward process. Noting that the statistical factor  $S$  is replaced by  $S' = \frac{1}{s} n(\mathbf{p}_3) n(\mathbf{p}_4) f_{K^-}(\mathbf{p}_K) [1 - n(\mathbf{p}_1)] [1 - n(\mathbf{p}_2)]$ , one obtains

$$\Gamma^{(\text{KT-B})}(\xi^{(\text{KT})}, T) = e^{\xi^{(\text{KT})}} \Gamma^{(\text{KT-F})}(\xi^{(\text{KT})}, T) \tag{28}$$

in the low temperature approximation.

The initial depletion of total strangeness is reflected in a negative value of  $\xi^{(\text{KT})}$ . Consequently, the production rate of thermal kaons through the forward KT reaction is larger than the annihilation rate through the backward reaction, as seen from (28). Eventually, when the system reaches chemical equilibrium where  $\xi^{(\text{KT})}=0$ , both the forward and the backward reaction rates become equal.

### III. EOS AND PHYSICAL CONDITIONS

In order to estimate the reaction rates, we must know for each chemical species the values of the physical quantities such as the chemical potential  $\mu_i$  and the number density  $n_i$  ( $i = n, p, e^-, K^-$ ), which depend on the specific physical properties of the system. As the initial condition ( $t=0$ ), we take normal neutron-star matter ( $\theta = 0$ ) which is composed of nonrelativistic neutrons ( $n$ ), protons ( $p$ ), and ultrarelativistic free electrons ( $e^-$ ) with a baryon number density  $n_B$ . The value of  $n_B$  is taken to be larger than the critical density for kaon condensation  $n_B^C$ . The initial kaon chemical potential  $\mu_K^0$  has a large negative value [see the latter part of this section], while  $\mu_e^0$  is positive.<sup>5</sup> Then the system is far from chemical equilibrium with  $\mu_e^0 \neq \mu_K^0$ , and evolves into a chemically equilibrated kaon-condensed phase. The temporal evolution of the kaon condensation proceeds through a set of rate equations which are given by the nonequilibrium weak reactions [28].

As for the EOS, the thermodynamic potential  $\Omega$  for the kaon-condensed phase is constructed with the help of chiral symmetry. Here we basically follow the result of [19] for  $\Omega$ . During the nonequilibrium processes, the time scales for the weak interactions are much larger than those for the strong and the electromagnetic interactions which are responsible for thermal equilibration. Therefore, the physical quantities are determined adiabatically under the assumption that the system is in thermal equilibrium, adjusting to the gradual change of the chemical compositions given by the weak interactions. Under this assumption, the corresponding values of  $\mu_i(t)$  and  $n_i(t)$  are related to each other,  $n_i(t) = -\partial\Omega(t)/\partial\mu_i(t)$ . Here we should note that both the zero-point and temperature fluctuations are simply neglected in the EOS except for the thermal contribution to the kaon number density, so that our expression for the EOS corresponds to the heavy-baryon limit in ref. [19] for the nucleons. On the other hand, to make clear the role of thermal kaons on the kinetics of condensation, we explicitly take into account the number of thermal kaons. Thus the kaon number density  $n_K$  is written as a sum of the condensed part  $\zeta_K$  and the thermal part  $n_K^T$ , as  $n_K(t) = \zeta_K(t) + n_K^T(t)$ , where

$$\zeta_K(t) \equiv \langle K^- | \hat{S} | K^- \rangle = \mu_K(t) f^2 \sin^2 \theta(t) + (1 - \cos \theta(t)) \left( n_p(t) + \frac{1}{2} n_n(t) \right) \quad (29)$$

with the strangeness operator,  $\hat{S} \equiv 2(\hat{Q} - \hat{I}_3 - \hat{B})$ ,

$$n_K^T(t) = \frac{1}{(2\pi)^3} \cos \theta \int d^3 p_K f_K(\mathbf{p}_K, t) \quad (30)$$

with

$$f_K(\mathbf{p}_K, t) = \frac{1}{e^{(\omega_-(t) - \mu_K(t))/T} - 1} - \frac{1}{e^{(\omega_+(t) + \mu_K(t))/T} - 1}, \quad (31)$$

and the first and second terms in the RHS of (31) are the Bose-Einstein distribution functions of the  $K^-$  and  $K^+$  mesons, respectively. It is to be noted that there appears a factor  $\cos \theta$  in the number density  $n_K^T(t)$ , which reduces to the noncondensed form in the limit of  $\theta \rightarrow 0$  ( $\cos \theta \rightarrow 1$ ) [19].

In the condensed phase, the expression for the  $\omega_{\pm}(\mathbf{p}_K)$  depends on how the fluctuations are incorporated [19,30]. Here we adopt the result by Tatsumi and Yasuhira [19]. The expression for  $\omega_{\pm}(\mathbf{p}_K)$  is then given by

---

<sup>5</sup>The superscript ‘0’ denotes the initial value at  $t = 0$ .

$$\omega_{\pm}(\mathbf{p}_K) = \pm \left\{ b + \mu_K (\cos \theta - 1) \right\} + \left[ \mathbf{p}_K^2 + (b^2 + \widetilde{m}_K^{*2}) \right]^{1/2}, \quad (32)$$

where  $b \equiv (n_p + \frac{1}{2}n_n)/(2f^2)$  with  $n_p$  ( $n_n$ ) the proton (neutron) number density, and  $\widetilde{m}_K^{*2} \equiv m_K^{*2} \cos \theta = (m_K^2 - n_B \Sigma_{KN}/f^2) \cos \theta$ , and  $\Sigma_{KN}$  is the  $KN$  sigma term. The term  $b$  stems from the  $KN$  vector interaction (the Tomozawa-Weinberg term), and  $m_K^{*2}$  is the effective kaon mass squared which is reduced due to the  $KN$  scalar interaction simulated by  $\Sigma_{KN}$  [11].

It may be seen from (32) that  $\omega_{-}(\mathbf{p}_K) \rightarrow \mu_K$  as  $\mathbf{p}_K \rightarrow 0$ , with the help of the classical field equation for  $\theta, \partial\Omega_K/\partial\theta = 0$  [11,19],

$$\sin \theta \left( \mu_K^2 \cos \theta + 2b\mu_K - m_K^{*2} \right) = 0. \quad (33)$$

In particular, in the condensed phase ( $\theta \neq 0$ ), the lowest excitation energy of the thermal kaons coincides with the kaon chemical potential. This Goldstone-like nature originates from the spontaneous  $V$ -spin symmetry breaking in the condensed phase. In the limit of  $\theta = 0$  in Eq.(32), one obtains an expression for the excitation energy of kaons in the normal phase. In this case, there is a gap between the lowest excitation energy  $\omega_{-}(\mathbf{p}_K = 0)$  and  $\mu_K$ .

For the EOS, the potential contribution of the symmetry energy,  $V_{\text{sym}}(n_B)$ , is taken into account in addition to the nonrelativistic Fermi-gas energy for the nucleons. Following Prakash et al. [31], we take the density dependence of  $V_{\text{sym}}(n_B)$  in the form

$$V_{\text{sym}}(n_B) = \left[ S_0 - (2^{2/3} - 1) \frac{3}{5} \epsilon_{F,0} \right] F(n_B), \quad (34)$$

where  $S_0 (= 30 \text{ MeV})$  is the empirical symmetry energy,  $\epsilon_{F,0}$  is the Fermi energy in the symmetric nuclear matter at  $n_0 (= 0.16 \text{ fm}^{-3})$ , the standard nuclear matter density, and  $F(n_B)$  is a function simulating the density dependence of  $V_{\text{sym}}(n_B)$ . For simplicity, we take  $F(n_B) = n_B/n_0$ . Then the chemical potential difference between the proton and the neutron in the condensed state is given by

$$\begin{aligned} \mu_p(t) - \mu_n(t) &= \frac{(3\pi^2 n_p(t))^{2/3}}{2m_N} - \frac{(3\pi^2 n_n(t))^{2/3}}{2m_N} + 4V_{\text{sym}}(n_B) \cdot (n_p(t) - n_n(t))/n_B \\ &\quad - \frac{1}{2}\mu_K(t)(1 - \cos \theta(t)), \end{aligned} \quad (35)$$

where  $n_p(t)$  ( $n_n(t)$ ) is the proton (neutron) number density [19].

With relevance to hot neutron stars at birth, we further assume that the system is initially in  $\beta$ -equilibrium, i.e.,  $\mu_n^0 = \mu_p^0 + \mu_e^0$ , due to the rapid  $\beta$ -decay reactions,  $n \rightarrow p + e^- + \bar{\nu}_e$ ,  $p + e^- \rightarrow n + \nu_e$ , and that the initial total strangeness is almost zero (with equal numbers of thermal  $K^{+}$ 's and  $K^{-}$ 's present). The latter condition means  $\mu_K^0 = -b^0$  as a consequence of Eqs.(30), (31), and (32) with  $\theta = 0$ . With these initial conditions, one can obtain the number densities  $n_i(t)$  from the rate equations, and then the chemical potentials  $\mu_i(t)$  and  $\theta(t)$  from Eqs.(33) and (35) together with the charge neutrality condition,

$$n_p(t) = n_e(t) + n_K(t). \quad (36)$$

Hereafter, we take the values for the effective nucleon mass ratios which appear in the expressions for the reaction rates to be  $m_p^*/m_N = m_n^*/m_N = 0.8$  for simplicity. The value for the  $KN$  sigma term is chosen to be  $\Sigma_{KN} = 300 \text{ MeV}$  as an example [32]. The critical density  $n_B^C$  is then estimated to be  $n_B^C = 0.485 \text{ fm}^{-3}$  ( $\sim 3.0 n_0$ ).

#### IV. NUMERICAL RESULTS AND DISCUSSION

In this section, we discuss the characteristic features of the forward KT reaction rate  $\Gamma^{(\text{KT-F})}(\xi^{(\text{KT})}, T)$ . The reaction rate  $\Gamma^{(\text{KT-F})}(\xi^{(\text{KT})}, T)$  is evaluated in the following two typical stages in the nonequilibrium process: (I) in an initial noncondensed state ( $\theta^0 = 0$ ,  $t=0$ ), and (II) in a condensed state in chemical equilibrium ( $\theta = \theta^{\text{eq}}$ ,<sup>6</sup>  $t \rightarrow \infty$ ).

(i) *Initial noncondensed state (I)*

First we consider a case with the baryon number density  $n_B = 0.55 \text{ fm}^{-3}$ , which is just above the critical density  $n_B^C$ . In this case, we take  $\mu_K^0 = -b^0 = -139 \text{ MeV}$ , and the initial proton-mixing ratio,  $x_p^0 \equiv n_p^0/n_B = 0.14$ . The initial values of the physical quantities are listed in Table I for the two baryon number densities. In Fig.2, the temperature dependence of  $\Gamma^{(\text{KT-F})}(\xi^{(\text{KT})}(0), T)$  is shown by the solid line. For comparison, the reaction rate for the forward MU process (MU-F) is shown by the dashed line (see Appendix A for the expression for the MU reaction rate). The MU-F reaction rate is taken for  $\beta$  equilibrium, i.e.,  $\xi^{(\text{MU})}(0) = 0$ . Note that there is no condensate yet at  $t = 0$ , so that the KU reactions cannot proceed. One can see that the magnitude of  $\Gamma^{(\text{KT-F})}(\xi^{(\text{KT})}(0), T)$  is large and dominates over that for MU,  $\Gamma^{(\text{MU-F})}(\xi^{(\text{MU})}(0) = 0, T)$ , over most cases except at very high temperature,  $T \gtrsim 5 \times 10^{11} \text{ K}$ . The large reaction rate for KT is due to the large deviation of the system from chemical equilibrium. For example, the value of  $\xi^{(\text{KT})}(0)$  is  $-4.6 \times 10^3/T_9 \ll 0$  at a relevant temperature  $T \lesssim 10^{11} \text{ K}$ . To see the  $\xi^{(\text{KT})}$ -dependence of  $\Gamma^{(\text{KT-F})}$ , we show the integrand  $f(x; u, T)$  of  $I^{(\text{KT-F})}(u, T)$  [ Eq.(26) ] in Fig.3 (a), as a function of  $x (= |\mathbf{p}_K|/T)$  with the temperature fixed at  $T = 1 \times 10^{11} \text{ K}$ . Several values of  $u$  are taken for comparison. In Fig.3 (b), the normalized kaon excitation energy  $\tilde{\omega}_- [= (\omega_-(x) - \mu_K)/T]$  is also shown. The value of  $f(x; u, T)$  for  $u = 0$ , in which case the normal neutron-star matter would be in chemical equilibrium without a kaon condensate, is much reduced, as is expected, because the energy gap measured from the chemical potential [ $\tilde{\omega}_-(x = 0) = (\omega_-(0) - \mu_K)/T > 0$ ] reduces the value of the Bose-Einstein distribution function [cf. Fig.3 (b) ]. However, as the value of  $u$  changes from zero to  $-100$ , the maximum value of  $f(x; u, T)$ ,  $f_{\text{max}}(u, T)$ , becomes larger by more than ten orders of magnitude. One can also see from Fig.3 (a) that the kaon momentum ( $x$ ) at  $f_{\text{max}}(u, T)$  becomes larger as  $|u|$  increases, and that a wider range of kaon momenta contribute to the integral  $I^{(\text{KT-F})}(u, T)$ . For the highly nonequilibrium case  $|u| \gtrsim 50$ , the main contribution to the reaction rate is associated with the hard thermal kaons with large momenta, rather than the soft kaons with  $\tilde{\omega}_-(x) - \tilde{\omega}_-(0) = O(1)$ , as seen in Fig.3 (b).

At lower temperatures,  $T \lesssim 10^{10} \text{ K}$ , the temperature dependence of the reaction rate  $\Gamma^{(\text{KT-F})}(\xi^{(\text{KT})}(0), T)$  is weak, as seen in Fig.2. In order to look into the details of this behavior, we show, in Fig.4, the integrand  $f(x; u = \xi^{(\text{KT})}(0), T)$  of  $I^{(\text{KT-F})}$  as a function of  $x$  with the input parameters  $\mu_K^0$  and  $x_p^0$  for  $n_B = 0.55 \text{ fm}^{-3}$  and for several temperatures,  $T = 10^8 - 10^{13} \text{ K}$ . One can see that, for  $T \lesssim 10^{10} \text{ K}$ ,  $f(x; u = \xi^{(\text{KT})}(0), T)$  is nearly proportional to  $x^4$  for  $x \lesssim x_M \equiv |\mathbf{p}_{K,M}|/T$ , where  $|\mathbf{p}_{K,M}|$  is the kaon momentum corresponding to a maximum of  $f$ . Above  $x = x_M$ , the integrand  $f$  decreases rapidly with  $x$ . This  $x$ -dependence of the integrand  $f(x; u = \xi^{(\text{KT})}(0), T)$  can be derived as follows: With the input parameters  $\mu_K^0$  and  $x_p^0$ , one finds  $\tilde{\omega}_-(x) \leq \tilde{\omega}_-(x_M) = 4.2 \times 10^3/T_9$  for  $x \leq x_M$ , and  $\xi^{(\text{KT})}(0) = -4.6 \times 10^3/T_9$ , so that  $\tilde{\omega}_-(x) + \xi^{(\text{KT})}(0) \lesssim -4 \times$

<sup>6</sup> The superscript ‘eq’ denotes the equilibrium value.

$10^2/T_9$  for  $x \leq x_M$ . Thus, one can show from Eq.(27) that  $f(x; u = \xi^{(\text{KT})}(0), T) \sim \frac{1}{6} \frac{x^4}{(\widetilde{\omega}_-(x) + \mu_K^0/T)^3} |\widetilde{\omega}_-(x) + \xi^{(\text{KT})}(0)|^3 \propto x^4$ , noting that  $|\widetilde{\omega}_-(x) + \xi^{(\text{KT})}(0)|^2 \gg 4\pi^2$  for  $T \lesssim 10^{10}$  K, and that the  $x$ -dependence of  $\widetilde{\omega}_-(x)$  is negligible for  $x \lesssim x_M$ . At a certain value of  $x$  just beyond  $x_M$ ,  $\widetilde{\omega}_-(x) + \xi^{(\text{KT})}(0)$  becomes positive, and the integrand  $f(x; u = \xi^{(\text{KT})}(0), T)$  decreases rapidly with  $x$  due to the exponential factor in (27), which originates from the statistical factor in the phase-space integrals of the reaction rate. Hence one obtains  $I^{(\text{KT-F})} \sim \int_0^{x_M} f dx \propto x_M^5$ . It is to be noted that the kaons which have the most dominant contribution to the KT reactions have momenta around a hundred MeV. For example, the value of the momentum  $|\mathbf{p}_{K,M}|$  is  $|\mathbf{p}_{K,M}| \simeq 120$  MeV for  $n_B = 0.55 \text{ fm}^{-3}$ . This kinematical range for the kaons is almost *independent* of the temperature as far as the temperature is low such that  $T \lesssim 10^{10}$  K (=0.86 MeV). Therefore,  $x_M (= |\mathbf{p}_{K,M}|/T)$  is simply proportional to  $T^{-1}$ , and  $I^{(\text{KT-F})} \propto T^{-5}$ . Thus one obtains  $\Gamma^{(\text{KT-F})}(\xi^{(\text{KT})}(0), T) = O(T^0)$  from Eq.(25b).

In the high temperature case,  $T \gtrsim 10^{12}$  K, on the other hand, the large energy of thermally excited kaons [ $T \gtrsim O(100 \text{ MeV})$ ] is comparable to the energy gap,  $\omega_-(\mathbf{p}_K = 0) - \mu_K$ , the latter of which is estimated to be 340 MeV for  $n_B = 0.55 \text{ fm}^{-3}$ . Thereby the soft kaons with energy less than the energy corresponding to  $\widetilde{\omega}_-(x) = O(1)$  contribute to the relevant reactions. For  $T \gtrsim 10^{12}$  K, a wide range of momenta of the thermal kaons give the main contribution to the reaction rate, and the value of  $|\mathbf{p}_{K,M}|$  depends sensitively on the temperature, as one can see in Fig.4.

(ii) *Condensed state in chemical equilibrium (II)*

For  $n_B = 0.55 \text{ fm}^{-3}$ , the input parameters in the equilibrated kaon-condensed phase are taken to be  $\theta^{\text{eq}} = 0.48$ ,  $\mu_K^{\text{eq}} = 203$  MeV, and  $x_p^{\text{eq}} = 0.23$ . The temperature dependence of the forward reaction rate  $\Gamma^{(\text{KT-F})}(\xi^{(\text{KT})}, T)$  with  $\xi^{(\text{KT})} = 0$  is shown in Fig.5 by the solid line for the baryon number density  $n_B = 0.55 \text{ fm}^{-3}$ , together with a plot of the forward KU process (KU-F) ( the MU-F process ) shown by the dotted line (dashed line). (see Appendix A for the expression for  $\Gamma^{(\text{KU-F})}$ .)

In order to discuss the kinematics for kaons in the KT reaction quantitatively, we show, in Fig.6,  $f(x; u = \xi^{(\text{KT})} = 0, T)$  and  $\widetilde{\omega}_-(x)$  for  $n_B = 0.55 \text{ fm}^{-3}$  and  $T = 10^9, 10^{10}$ , and  $10^{11}$  K. One can see that the maximum of  $f(x; u = \xi^{(\text{KT})} = 0, T)$  corresponds to  $\widetilde{\omega}_-(x) = a = O(1)$ , where  $a = 2 - 3$ , i.e., *soft thermal kaons* with thermal energies produce a dominant contribution to the KT reaction in the condensed phase.<sup>7</sup> This feature holds for all temperatures. By expanding  $\widetilde{\omega}_-(x)$  with respect to the kaon momentum  $|\mathbf{p}_K|$  by the use of the classical field equation, Eq.(33), one obtains the momentum  $|\mathbf{p}_{K,M}|$  corresponding to the maximum of the integrand,  $f_{\text{max}}$ , as

$$|\mathbf{p}_{K,M}| = \sqrt{2a(b^{\text{eq}} + \mu_K^{\text{eq}} \cos \theta^{\text{eq}})T} \propto T^{1/2} \quad (37)$$

for the temperatures  $T \lesssim 10^{11}$  K, or  $x_M = |\mathbf{p}_{K,M}|/T \propto T^{-1/2}$ . The temperature-dependence of  $f_{\text{max}}$  is then written roughly as

$$f_{\text{max}} \sim \frac{1}{6} \frac{[2a(b^{\text{eq}} + \mu_K^{\text{eq}} \cos \theta^{\text{eq}})]^2}{T^2(a + \mu_K^{\text{eq}}/T)^3} \frac{a}{1 - e^{-a}} \frac{(a^2 + 4\pi^2)}{e^a - 1}. \quad \text{In the low temperature limit, } \mu_K^{\text{eq}}/T \gg a, \text{ which gives } f_{\text{max}} \propto T. \text{ In this case, } I^{\text{KT-F}}(\xi^{(\text{KT})} = 0, T) \sim f_{\text{max}} \Delta x \propto T^{1/2},$$

<sup>7</sup>The importance of thermal loops in the soft (Goldstone) mode for the phase diagram and EOS has been also emphasized in ref. [19].

where  $\Delta x (= \Delta p_K/T)$  is the dominant integration range around  $x_M$ . Hence one finds  $\Gamma^{(\text{KT-F})}(\xi^{(\text{KT})} = 0, T) \propto T^{5.5}$ .

At temperatures below  $\sim 10^8$  K, the reaction rate for KT,  $\Gamma^{(\text{KT-F})}(\xi^{(\text{KT})} = 0, T)$ , is less than that for KU,  $\Gamma^{(\text{KU-F})}(\xi^{(\text{KU})} = 0, T)$ . Nevertheless, since the temperature dependence of the KT process ( $\propto T^{5.5}$ ) is more pronounced than that for the KU process ( $\propto T^5$ ), the reaction rate  $\Gamma^{(\text{KT-F})}(\xi^{(\text{KT})} = 0, T)$  increases more rapidly as a function of the temperature than  $\Gamma^{(\text{KU-F})}(\xi^{(\text{KU})} = 0, T)$ , and the former exceeds the latter for  $T \gtrsim 10^8$  K. At temperatures  $T \gtrsim 10^9$  K,  $\Gamma^{(\text{KT-F})}(\xi^{(\text{KT})} = 0, T)$  is larger than  $\Gamma^{(\text{KU-F})}(\xi^{(\text{KU})} = 0, T)$  by one or two orders of magnitude, and at temperatures below  $\sim 4 \times 10^{11}$  K,  $\Gamma^{(\text{KT-F})}(\xi^{(\text{KT})} = 0, T)$  is also larger than  $\Gamma^{(\text{MU-F})}(\xi^{(\text{MU})} = 0, T)$ .

(iii) *Comparison between cases (I) and (II)*

Next we compare the reaction rate for KT in the case (I) with that in the case (II) (cf. Figs.2 and 5). The former is larger than the latter for all the temperatures. For example, the former is large in magnitude by a factor  $\sim 10^6$  at  $T = 10^{10}$  K, and this factor becomes much more significant at lower temperatures, where hard thermal kaons with  $\widetilde{\omega}_-(x) \gg 1$  take part in an enhancement of the KT reactions in the nonequilibrium state. As the temperature increases, the ratio,  $\Gamma^{(\text{KT-F})}[\text{case (II)}]/\Gamma^{(\text{KT-F})}[\text{case (I)}]$ , becomes smaller, and tends to have a  $T$  dependence similar to each other at very high temperatures,  $T \gtrsim 10^{12}$  K, where soft kaons with energies  $\widetilde{\omega}_-(x) = O(1)$  become responsible for the reactions KT for both (I) and (II).

(iv) *Comparison at different densities*

Finally, in Fig.7, we show the temperature dependence of the relevant forward reaction rates for  $n_B=0.70 \text{ fm}^{-3}$ . At this density, we have the fully-developed kaon-condensed phase after chemical equilibrium is attained. The values for the parameters are estimated to be  $\mu_K^0 = -b^0 = -180 \text{ MeV}$  and  $x_p^0=0.16$  for the case (I), and  $\theta^{\text{eq}}=0.91$ ,  $\mu_K^{\text{eq}}=114 \text{ MeV}$ , and  $x_p^{\text{eq}}=0.39$  for the case (II). Figure 7 (a) [ Fig.7 (b) ] is for the case (I) [case (II) ]. The qualitative features are the same as those at a lower density  $n_B=0.55 \text{ fm}^{-3}$ , although there is a significant increase in the magnitude of the KT reaction rate at the same temperature as compared with the lower density case of  $n_B=0.55 \text{ fm}^{-3}$  [ cf. Fig.2 for (I) and Fig.5 for (II) ].

In the initial noncondensed case (I), the value of  $\xi^{(\text{KT})}(0)$  is further reduced to  $\xi^{(\text{KT})}(0) = -5.5 \times 10^3/T_9$  with increase in density, because the decrease in  $\mu_K^0$  and the increase in  $\mu_e^0$  enlarge the value of  $|\xi^{(\text{KT})}(0)| (= |\mu_e^0 - \mu_K^0|/T)$ . This difference in  $\xi^{(\text{KT})}(0)$  becomes important in determining the magnitude of the KT reaction rate for temperatures  $T \lesssim 10^{11}$  K. For example, the ratio of the reaction rates at different densities,  $r(\text{I}) = \Gamma^{(\text{KT-F})}(0.70 \text{ fm}^{-3})/\Gamma^{(\text{KT-F})}(0.55 \text{ fm}^{-3})$ , becomes  $r(\text{I}) \sim 10^3$  for  $T \lesssim 10^{10}$  K. For temperatures as high as  $T \gtrsim 5 \times 10^{11}$  K, the difference in  $\xi^{(\text{KT})}(0)$  becomes less significant because  $|\xi^{(\text{KT})}(0)| \lesssim 10$  at both densities, so that the ratio becomes small:  $r(\text{I}) = \Gamma^{(\text{KT-F})}(0.70 \text{ fm}^{-3})/\Gamma^{(\text{KT-F})}(0.55 \text{ fm}^{-3}) \lesssim 10$  for  $T \gtrsim 5 \times 10^{11}$  K.

On the other hand, in the case of the condensed state in chemical equilibrium (II), the ratio  $r(\text{II}) = \Gamma^{(\text{KT-F})}(0.70 \text{ fm}^{-3})/\Gamma^{(\text{KT-F})}(0.55 \text{ fm}^{-3}) \sim 3$  at low temperatures  $T \lesssim 10^{10}$  K, while  $r(\text{II})$  becomes less than 2 at high temperatures  $T \gtrsim 5 \times 10^{11}$  K. This enhancement with increase in density mainly stems from the reduction in the kaon chemical potential  $\mu_K^{\text{eq}}$ , which appears in the denominator of the function  $f(x; u = \xi^{(\text{KT})} = 0, T)$ : In the kaon-condensed phase,  $\mu_K^{\text{eq}}$  decreases monotonically as the density increases [13] such that  $\mu_K^{\text{eq}}=203 \text{ MeV} \rightarrow 114 \text{ MeV}$  as  $n_B=0.55 \text{ fm}^{-3} \rightarrow 0.70 \text{ fm}^{-3}$ . At low temperatures, the term  $\mu_K^{\text{eq}}/T$  is larger than  $\widetilde{\omega}_-(x) (= O(1))$  in the factor  $1/(\widetilde{\omega}_-(x) + \mu_K^{\text{eq}}/T)^3$ , so that  $r(\text{II})$  is mainly determined by  $[\mu_K^{\text{eq}}(0.55 \text{ fm}^{-3})/\mu_K^{\text{eq}}(0.70 \text{ fm}^{-3})]^3$ . At high temperatures, the term  $\mu_K^{\text{eq}}/T$  is

less significant, so that the difference of the integral  $I^{(\text{KT-F})}(\xi^{(\text{KT})} = 0, T)$  between the different densities is less marked.

## V. SUMMARY AND CONCLUDING REMARKS

We have calculated the reaction rates for the thermal kaon (KT) process. We based on chiral symmetry as a guiding principle in obtaining the excitation energy of the kaons and the transition matrix element for the reaction rates. It has been shown that the reaction rate is larger than those of the kaon-induced Urca (KU) and the modified Urca (MU) reactions for the relevant temperatures and baryon number densities which may be realized in the early hot stage of neutron stars. The KT process is dominant not only in the case of the noncondensed state, which is in a highly nonequilibrium state ( $|\xi^{\text{KT}}(t)| \gg 1$ ), but also in the case of the kaon-condensed state in chemical equilibrium ( $|\xi^{\text{KT}}(t)| = 0$ ). In the noncondensed state, where there is a gap between the minimum excitation energy and the kaon chemical potential, it is mainly hard thermal kaons with large momenta, rather than soft thermal kaons, which contribute to the reaction rate. On the other hand, in the condensed state, the soft kaon mode  $[\omega_-(\mathbf{p}_K) - \mu_K = O(T)]$ , which reflects the spontaneously broken  $V$ -spin symmetry, contributes to the reaction rate. We have seen that the hard and soft kaons contribute differently, which results in a different temperature dependence for the reaction rates in the noncondensed and condensed states.

The KT reactions are found to be dominant throughout the nonequilibrium process, and may control the characteristic time scales, such as those for the onset of condensation and its subsequent buildup. Dynamical evolution of the kaon-condensed state can be treated by pursuing temporal changes in the condensation by way of a set of kinetic equations, where the chemical species change through the nonequilibrium weak reactions. This subject will be discussed in detail elsewhere [28].

In addition, there are several astrophysical implications of the present work. First, Brown and Bethe [14] have proposed a scenario in which low-mass black holes are formed in stellar collapse using a very soft equation of state due to kaon condensation. Following this scenario, Baumgarte et al. made a dynamical simulation of the delayed collapse of a hot neutron star to a black hole [16]. They utilized the nuclear EOS with kaon condensation in the equilibrium configuration at  $T = 0$ . However, there might be a time lag for the appearance and growth of a condensate due to the nonequilibrium weak reactions, even when the density exceeds the critical density for the condensation. Hence one needs to treat the nonequilibrium processes for a careful consideration of the dynamical evolution of an initially normal neutron star to a kaon-condensed star. Second, nonequilibrium weak reactions may also affect the stability of neutron stars near the maximum mass with respect to a perturbation from their static configurations [33]. For normal nuclear matter, the  $\beta$  processes (3) have been taken into account as the most important weak reactions [33]. For kaon-condensed matter, the KT process is expected to be the most relevant reactions for stability. Third, as another dynamical property related to neutron stars, mechanisms for the dissipation of the vibrational energy of neutron stars induced by nonequilibrium weak reactions have been discussed for several phases of hadronic matter [34]. The associated bulk viscosity determines the damping time scale for radial oscillations of neutron stars. In a kaon condensate, the KT reactions may be most effective for dissipation, and may have a major contribution to the damping of the radial oscillations of kaon-condensed stars.

## VI. ACKNOWLEDGEMENTS

The authors wish to thank Professor R.T.Deck for comments on the manuscript. One of the authors (T.M.) is indebted for the Grant-in-Aid of Chiba Institute of Technology (C.I.T). Part of the numerical calculations was performed by the use of the DEC Alpha Server 4100 System in C.I.T. This material is based upon work supported in part by the National Science Foundation through the Theoretical Physics Program under Grant Nos.PHY9008475 and PHY9722138, and by the Japanese Grant-in-Aid for Scientific Research Fund of the Ministry of Education, Science, Sports and Culture (08640369, 11640272).

### APPENDIX A: OTHER WEAK REACTIONS

For comparison, we here list other relevant weak reactions KU and MU, which may be operative in the nonequilibrium process in kaon condensation.

The KU reactions are mediated by the last term (the ‘‘commutator’’ contribution) in Eq.(9). The reaction rate for the forward KU process (2a), is given as

$$\begin{aligned}\Gamma^{(\text{KU-F})}(\xi^{(\text{KU})}, T) &= \frac{G_F^2}{64\pi^5} \sin^2 \theta_C \sin^2 \theta \left\{ 10 + 3(g_A^2 + 9\tilde{g}_A^2) \right\} m_N^{*2} \mu_e T^5 I_2(\xi^{(\text{KU})}) \\ &= (6.6 \times 10^{29}) \left( \frac{m_N^*}{m_N} \right)^2 \frac{\mu_e}{m_\pi} \sin^2 \theta T_9^5 I_2(\xi^{(\text{KU})}) \text{ (cm}^{-3} \cdot \text{s}^{-1})\end{aligned}\quad (\text{A1})$$

where  $\tilde{g}_A = F - \frac{1}{3}D=0.15$  with  $F + D = g_A = 1.25$  and  $D/(D + F) = 0.658$  [13],  $I_2(u) \equiv \int_0^\infty dx x^2 [\pi^2 + (x + u)^2] / (1 + \exp(x + u))$  and  $\xi^{(\text{KU})} \equiv (\mu_e - \mu_K)/T$ .

For the MU reaction, we refer to Haensel’s result [35] which is based on [24]. Noting that the matrix elements are slightly modified in the presence of the kaon-condensate by an additional factor of  $\cos^2(\theta/2)$  coming from the first term in the first curly brackets for the isospin-changing strangeness-conserving current in (9), one obtains

$$\Gamma^{(\text{MU-F})}(\xi^{(\text{MU})}, T) = (5.9 \times 10^{23}) \left( \frac{n_e}{n_0} \right)^{1/3} \cos^2 \frac{\theta}{2} T_9^7 J_2(\xi^{(\text{MU})}) \text{ (cm}^{-3} \cdot \text{s}^{-1}) , \quad (\text{A2})$$

where  $J_2(u) \equiv \int_0^\infty dx x^2 [9\pi^4 + 10\pi^2(x + u)^2 + (x + u)^4] / (1 + \exp(x + u))$ , and  $\xi^{(\text{MU})} \equiv (\mu_p + \mu_e - \mu_n)/T$ .

For the backward processes, one can see  $\Gamma^{(\text{KU-B})} = \Gamma^{(\text{KU-F})}(-\xi^{(\text{KU})})$ ,  $\Gamma^{(\text{MU-B})} = \Gamma^{(\text{MU-F})}(-\xi^{(\text{MU})})$  within the low-temperature approximation. It is to be noted that the relation between the forward and backward reaction rates for KT [ (28) ] is different from that for KU or MU due to the appearance of the Bose-Einstein distribution function in the phase-space integrals for KT.



## REFERENCES

- [1] D. B. Kaplan and A. E. Nelson, Phys. Lett.**B175**, 57 (1986);**B179**, 409(E) (1986).  
A. E. Nelson and D. B. Kaplan, Phys. Lett.**B192**, 193 (1987).
- [2] T. Tatsumi, Prog. Theor. Phys.Suppl. **120**,111 (1995).
- [3] C. -H. Lee, Phys. Rep.**275**,197 (1996).
- [4] G. E. Brown, C.- H. Lee and R. Rapp, Nucl. Phys.**A639**,455c(1998).
- [5] T. Waas,N. Kaiser and W. Weise, Phys. Lett.**B365**,12(1996); **B379**,34(1996).  
T. Waas and W. Weise, Nucl.Phys.**A625**,287(1997).
- [6] M. Lutz, Phys. Lett.**B426**,12(1998).
- [7] C. J. Batty, E. Friedman and A. Gal, Phys.Rep.**287**,385(1997).
- [8] R. Barth et al., Phys. Rev. Lett.**78**,4007(1997).
- [9] F. Laue et al., Phys. Rev. Lett.**82**,1640(1999).
- [10] G. Song, B.- A. Li and C. M. Ko, Nucl. Phys.**A646**,481(1999).
- [11] H. Fujii, T. Maruyama, T. Muto and T. Tatsumi, Nucl. Phys.**A597**,645 (1996).
- [12] T. Tatsumi, Prog. Theor. Phys.**80**,22 (1988).
- [13] H. Fujii, T. Muto, T. Tatsumi and R. Tamagaki, Nucl.Phys.**A571**,758 (1994);  
Phys. Rev.**C50**, 3140 (1994).
- [14] G. E. Brown and H. A. Bethe, Astrophys.J.**423**, 659 (1994).
- [15] M. Prakash, I. Bombaci, M. Prakash, P. J. Ellis, J. M. Lattimer, R. Knorren, Phys.  
Rep. **280**, 1(1997).
- [16] T. W. Baumgarte, S. L. Shapiro and S. Teukolsky, Astrophys. J. **443**, 717 (1995);  
**458**, 680 (1996).
- [17] W. Keil and H.-Th. Janka, Astron.Astrophys. **296**,145(1995).
- [18] J. A. Pons, et al, Astrophys.J.**513**,780(1999).
- [19] T. Tatsumi, KUNS 1483 (1997); T. Tatsumi and M. Yasuhira, Phys.Lett. **B441**,9  
(1998); Nucl.Phys.**A** in press (nucl-th/9811067).
- [20] T. Tatsumi and M. Yasuhira, nucl-th/9904038.
- [21] *Bose-Einstein Condensation*, edited by A. Griffin, D. W. Snoke, and S. Stringari,  
(Cambridge University Press, New York,1995).
- [22] E. Levich and V. Yakhot, J.Phys.**B15**, 243 (1977).  
U. Eckern, J.Low Temp. Phys.**54**, 333 (1984).  
D. W. Snoke and J. P. Wolfe, Phys.Rev.**B39**, 4030 (1989).  
H. T. C. Stoof, Phys.Rev.Lett.**66**, 3148 (1990); Phys.Rev.**A45**, 8398 (1992).  
Yu. M. Kagan, B. V. Svistunov, and G. V. Shlyapnikov, Sov.Phys. JETP**74**, 279  
(1992).  
D. V. Semikoz and I. I. Tkachev, Phys.Rev.Lett.**74**,3093 (1995); and references  
therein.  
For a recent theoretical review, F. Dalfovo, S. Giorgini, L. P. Pitaevskii, and  
S.Stringari, Rev.Mod.Phys.**71**, 463(1999).
- [23] M. H. Anderson et al., Science **269**,198 (1995).  
C. C. Bradley,C. A. Sackett, J. J. Tollett, and R. G. Hulet, Phys.Rev.Lett.**75**,1687  
(1995).  
K. B. Davis et al., Phys.Rev.Lett.**75**, 3969 (1995).
- [24] B. L. Friman and O. V. Maxwell, Astrophys.J.**232**, 541(1979).
- [25] O. V. Maxwell, Astrophys.J.**316**,691(1987).
- [26] S. K. Ghosh, S. C. Phatak and P. K. Sahu, Nucl.Phys.**A596**, 670 (1996).
- [27] T. Muto, T. Tatsumi, and N. Iwamoto, Aust. J. Phys. **50**, 13 (1997).

- [28] T. Muto, T. Tatsumi, and N. Iwamoto, preprint (1999) (paper II).
- [29] G. Baym and C. J. Pethick, *Landau Fermi-Liquid Theory* (Wiley, New York, 1991).
- [30] V. Thorsson and P. J. Ellis, Phys. Rev. **D55**, 5177 (1997).
- [31] M. Prakash, T. L. Ainsworth and J. M. Lattimer, Phys. Rev. Lett. **61**, 2518(1988).
- [32] J. F. Donoghue and C. R. Nappi, Phys. Lett. **B168**, 105 (1986).  
R. L. Jaffe and C. L. Korpa, Commun. Nucl. Part. Phys. **17**, 163 (1987).
- [33] E. Gourgoulhon, P. Haensel, and D. Gondek, Astron. Astrophys. **294**, 747 (1995).
- [34] C. Cutler, L. Lindblom, and R. J. Splinter, Astrophys. J. **363**, 603 (1990).
- [35] P. Haensel, Astron. Astrophys. **262**, 131 (1992).

## TABLES

TABLE I. Input quantities for the initial noncondensed state ( $t = 0$ ) and for the chemical equilibrated state ( $t \rightarrow \infty$ ). All the values are estimated at  $T=0$ . The former (the latter) quantities are denoted by the superscript ‘0’ ( ‘eq’ ).

$n_B(\text{fm}^{-3})$	$\mu_K^0$ ( MeV )	$x_p^0$	$\theta^{\text{eq}}$ (rad)	$\mu_K^{\text{eq}}$ ( MeV )	$x_p^{\text{eq}}$
0.55	-139	0.14	0.48	203	0.23
0.77	-180	0.16	0.91	114	0.39

FIGURES

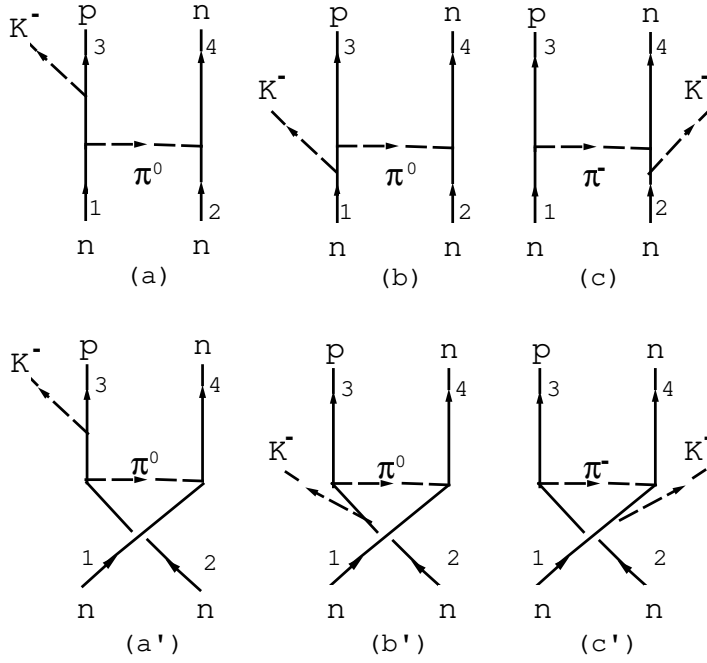


FIG. 1. The lowest-order diagrams for the reactions (1a) that produce the thermal kaons.

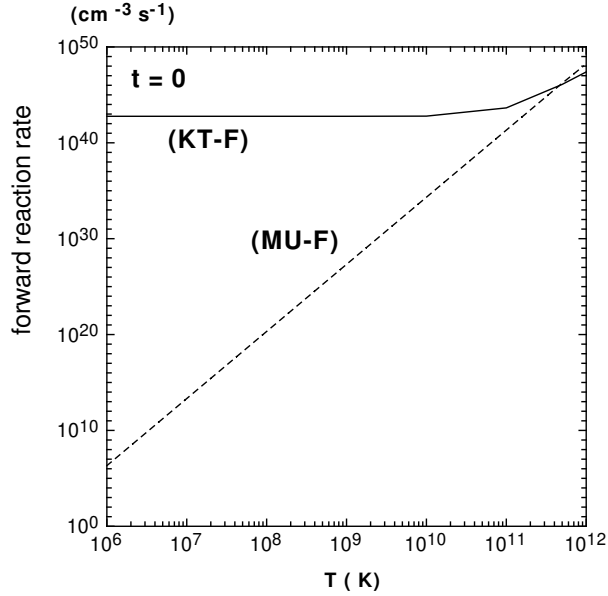


FIG. 2. Temperature dependence of the forward KT reaction rate  $\Gamma^{(\text{KT-F})}(\xi^{(\text{KT})}(0), T)$  at an initial noncondensed stage [case (I)] for  $n_B=0.55 \text{ fm}^{-3}$  (solid line). For comparison, the plot for the forward MU reaction rate is shown by the dashed line.

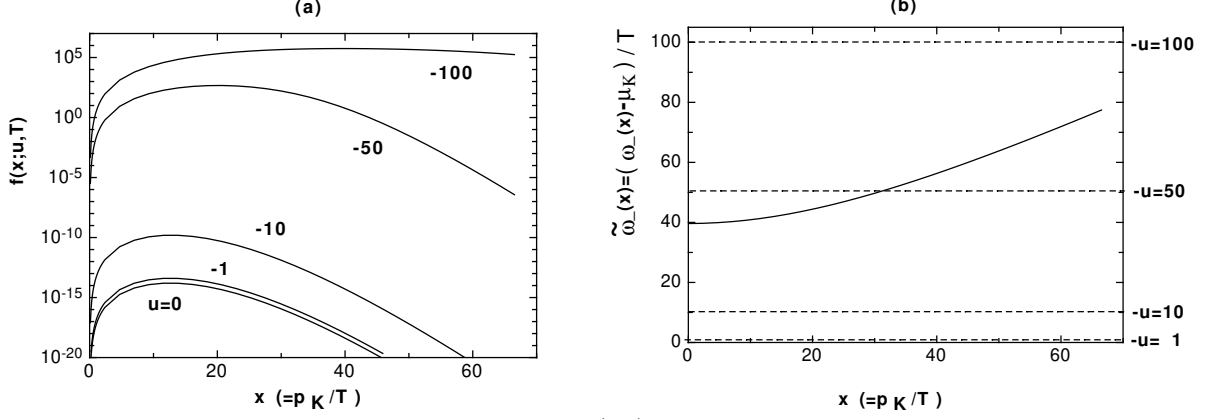


FIG. 3. (a) Function  $f(x; u, T)$  in the integrand  $I^{(KT)}(u, T)$  for the KT-F reaction rate as a function of  $x (= |\mathbf{p}_K|/T)$  for several values of  $u$  at an initial noncondensed stage (case (I)). The result is for  $n_B=0.55 \text{ fm}^{-3}$  and  $T = 1.0 \times 10^{11} \text{ K}$ . (b)  $\tilde{\omega}_-(x) [= (\omega_-(x) - \mu_K)/T]$ , the kaon excitation energy normalized by the temperature under the same condition as in Fig.3(a).

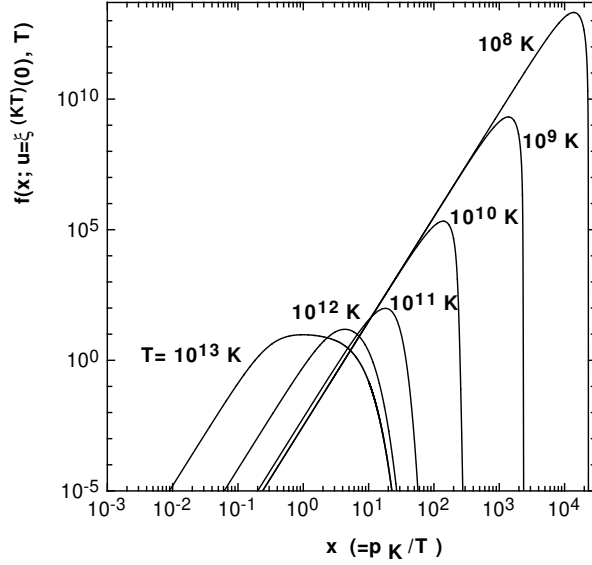


FIG. 4. The integrand  $f(x; u = \xi^{KT}(0), T)$  of  $I^{(KT-F)}$  as a function of  $x$  with the input parameters  $\mu_K^0$  and  $x_p^0$ , for  $n_B=0.55 \text{ fm}^{-3}$  and for several temperatures,  $T = 10^8 - 10^{13} \text{ K}$ .

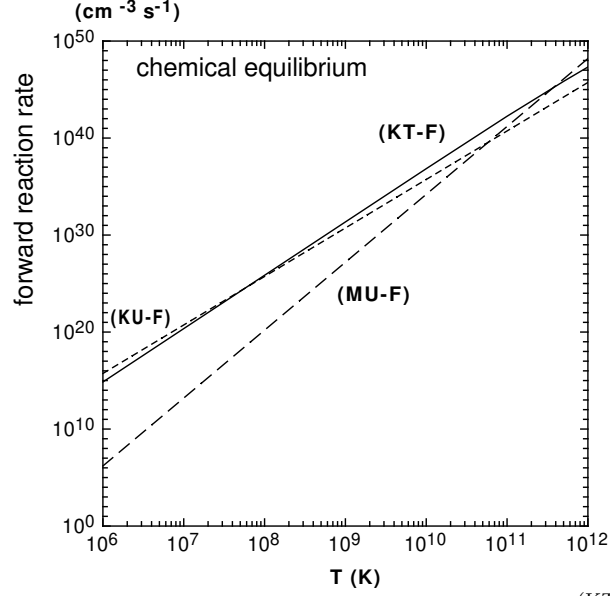


FIG. 5. Temperature dependence of the forward KT reaction rate  $\Gamma^{(\text{KT-F})}(\xi^{(\text{KT})} = 0, T)$  in the kaon-condensed phase in chemical equilibrium (II) for  $n_B=0.55\text{fm}^{-3}$  (solid line). For comparison, the reaction rate for the KU process (the MU process) is shown with a dotted line (dashed line).

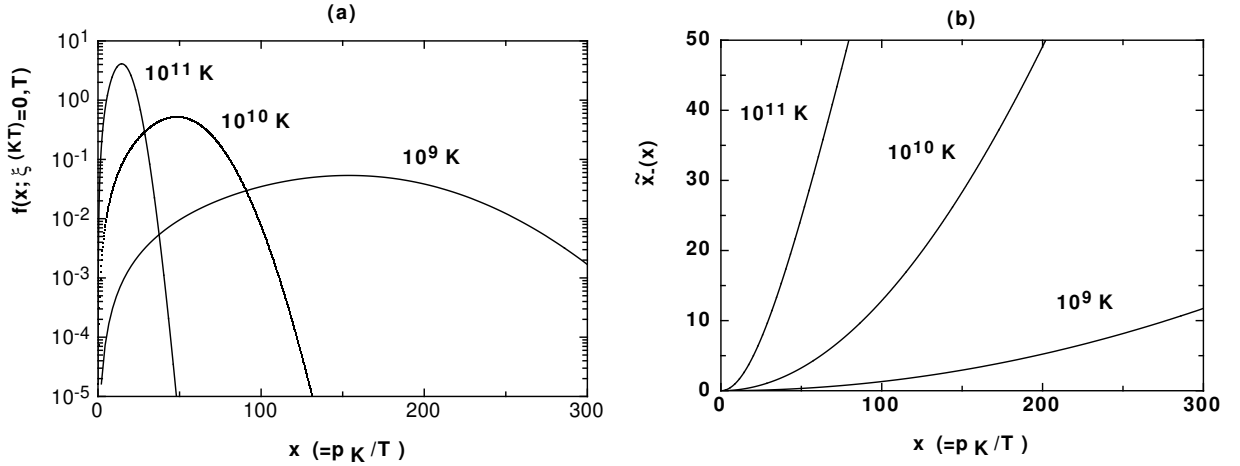


FIG. 6. (a) Function  $f(x; u = \xi^{(\text{KT})} = 0, T)$  at the equilibrated  $K^-$ -condensed stage (II) as a function of  $x$  for  $n_B=0.55\text{fm}^{-3}$  and several temperatures.

(b)  $\tilde{\omega}_-(x)$  as a function of  $x$  under the same condition as Fig.6(a).

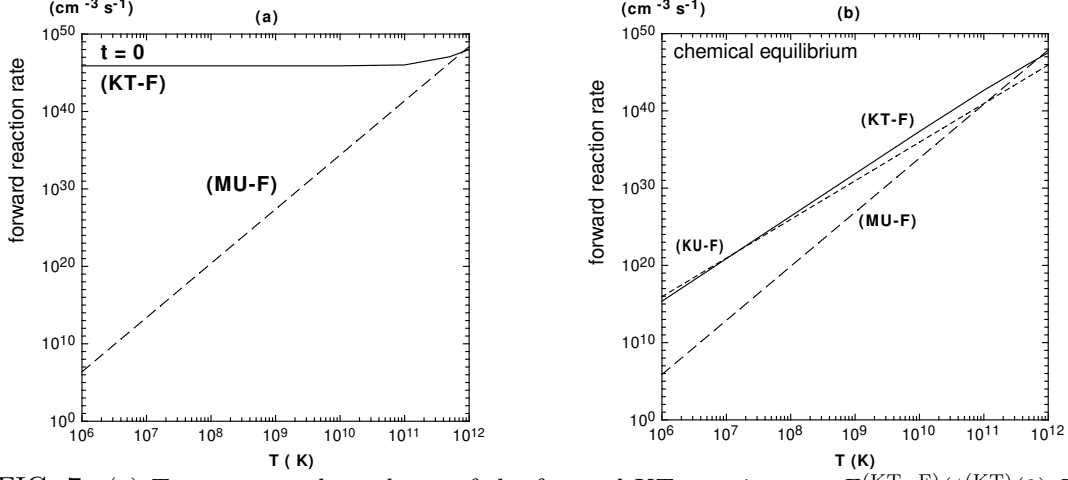


FIG. 7. (a) Temperature dependence of the forward KT reaction rate  $\Gamma^{(KT-F)}(\xi^{(KT)}(0), T)$  at an initial noncondensed stage [case (I)] for  $n_B=0.70\text{fm}^{-3}$  (solid line). For comparison, the plot for the forward MU reaction is shown by the dashed line.

(b) Temperature dependence of the forward KT reaction rate  $\Gamma^{(KT-F)}(\xi^{(KT)} = 0, T)$  in the kaon-condensed phase in chemical equilibrium [case (II)] for  $n_B=0.70\text{fm}^{-3}$  (solid line). For comparison, the rate for the KU process (the MU process) is shown by the dotted line (dashed line).